Acta Cryst. (1997). B53, 444–450

Zeolite Rho Loaded with Methylamines. III. Trimethylamine Loadings

CLAUDIA WEIDENTHALER,[a] REINHARD X. FISCHER,[a]* LLOYD ABRAMS[b] AND ALAN HEWAT[c]

[a]*Fachbereich Geowissenschaften der Universität,† Klagenfurter Strasse, D-28359 Bremen, Germany,* [b]*Central Research and Development Department,‡ EI du Pont de Nemours & Co., Experimental Station, Wilmington, DE 19880, USA, and* [c]*Institut Laue–Langevin, F-38042 Grenoble CEDEX 9, France. E-mail: rfischer@min.uni-bremen.de*

(Received 3 May 1996; accepted 7 October 1996)

Abstract

Samples of two differently prepared zeolites rho loaded with different amounts of trimethylamine (TMA) were studied in their hydrated and dehydrated forms by X-ray and neutron diffraction experiments. Both zeolites are partially dealuminated, as indicated by nonframework Al, which is assumed to be Al_2O_3 or AlOOH. Series I was prepared from dry-calcined NH_4-rho at 873 K, series II from steam-calcined NH_4-rho at 773 K. The samples were loaded with different amounts of deuterated TMA. Rietveld refinements yielded the following results for series I: (1) $H_{3.8}(H\text{-}TMA)_5Cs_{0.2}Al_9Si_{39}O_{96}.Al_2O_3.22H_2O$, X-ray data collection at room temperature, $Im\bar{3}m$, a = 15.0542 (2) Å, R_{wp} = 0.094; (2) composition as in (1) (anhydrous), neutron data collection at 5 K of dehydrated and deuterated sample, $Im\bar{3}m$, a = 15.0467 (4) Å, R_{wp} = 0.034. Series II: (3) $H_{0.3}(H\text{-}TMA)_5Cs_{0.7}Al_6Si_{42}O_{96}.2.5Al_2O_3.22H_2O$, X-ray data collection at room temperature, $Im\bar{3}m$, a = 15.0574 (2) Å, R_{wp} = 0.118; (4) composition as in (3) (anhydrous), neutron data collection at 5 K of dehydrated and deuterated sample, $Im\bar{3}m$, a = 15.0761 (5) Å, R_{wp} = 0.037. In all determinations the TMA molecules reside with the N and H (D in neutron diffraction analysis) atoms on the central axes (x, 0, 0) pointing towards the center of the single eight-ring, whilst the three methyl groups point away to the center of the α-cage.

1. Introduction

The third part of our studies of methylamine-loaded zeolites rho is concerned with trimethylamine (TMA) modifications. TMA is produced in the synthesis of dimethylamine (DMA) from the reaction of methanol and ammonia (Keane, Sonnichsen, Abrams, Corbin, Gier & Shannon, 1987). Zeolite rho is used as a shape-selective catalyst with a DMA production rate approximately corresponding to the commercial methylamine demand. While the small molecules of monomethylamine (MMA) and DMA easily diffuse through the zeolite channel system, the larger TMA molecules are trapped in the cages. They are extracted from the zeolite at elevated temperatures following the reaction scheme with a decomposition of TMA according to (Abrams, Corbin & Keane, 1990)

$$\underset{\text{TMA}}{(CH_3)_3N} \rightarrow \underset{\text{DMA}}{(CH_3)_2NH} + CH_2 \rightarrow \underset{\text{MMA}}{CH_3NH_2} + CH_2.$$

DMA and TMA selectivities depend strongly on the method and temperature of calcination of the NH_4-rho precursor (Shannon, Keane, Abrams, Staley, Gier, Corbin & Sonnichsen, 1988). This paper describes the crystal chemical influence of the TMA molecules upon sorption in two differently prepared samples of zeolite rho.

2. Experimental

All samples were prepared as described in the first paper of this series. One sample of zeolite rho deammoniated under dry nitrogen at 873 K (series I) and one sample of steam-calcined rho at 773 K (series II) were loaded with deuterated TMA to give approximately five molecules per unit cell after dehydration of the zeolites. The numbers of sorbed molecules, as determined by thermal analyses, are given in Table 1. Thermal analyses, X-ray and neutron diffraction experiments, and Rietveld analyses were performed with the equipment and programs described in the first article on MMA-rho.†

2.1. *Thermal analyses*

Fig. 1 shows the thermal reactions and weight losses upon heating to 973 K. Decomposition of the TMA molecules is indicated by the exothermic reactions above 573 K after dehydration at *ca* 373 K. Rho-I-5TMA exhibits a maximum TMA decomposition at

† Part of this work was done at the Institut für Geowissenschaften der Universität Mainz, Germany.

‡ Contribution No. 7367.

† The numbered intensity of each measured point on the profile has been deposited with the IUCr (Reference: SE0201). Copies may be obtained through The Managing Editor, International Union of Crystallography, 5 Abbey Square, Chester CH1 2HU, England.

Table 1. *Methylamine (MA) loadings in the zeolite rho samples*

Series I: Shallow bed calcined at 873 K under dry nitrogen, water content determined by TG analysis in the temperature range between room temperature and 673 K, methylamine content between 673 and 973 K; series II: Shallow bed calcined under steam at 773 K, water determined between room temperature and 573 K, methylamine content between 573 and 1073 K.

Sample series	Initial loading (no. per unit cell)	Weight loss of H_2O (mg)	No. of H_2O per unit cell	Weight loss of MA (mg)	No. of MA per unit cell	Desorption temperature (K)
Rho-I	5 TMA	5.3	22.3	4.7	5.9	703
Rho-II	5 TMA	4.8	21.8	3.0	4.0	613/643

703 K similarly to Rho-I-5DMA (Weidenthaler, Fischer & Abrams, 1997). The sample of series II shows three resolved exothermic reactions in this temperature range, again similarly to the corresponding DMA sample Rho-II-5DMA, but more pronounced. The broader exothermic feature at *ca* 873 K might indicate the burn-off of the coke residue.

2.2. *Rietveld analyses*

The two samples were studied in their hydrated forms by X-ray diffraction and for the dehydrated and deuterated forms by neutron diffraction. The letters X and N behind the sample designations refer to X-ray and neutron diffraction studies, respectively. The N- and C-atom coordinates for TMA were refined with restraints on the intramolecular bonds prescribed by 1.4535 Å for C—N, 2.387 Å for C—C and 110.4° for the C—N—C angles taken from Blake, Ebsworth & Welch (1984) in a combined distance least-squares (DLS) and Rietveld refinement. Unit-cell data and residuals for all refinements are given in Table 2.

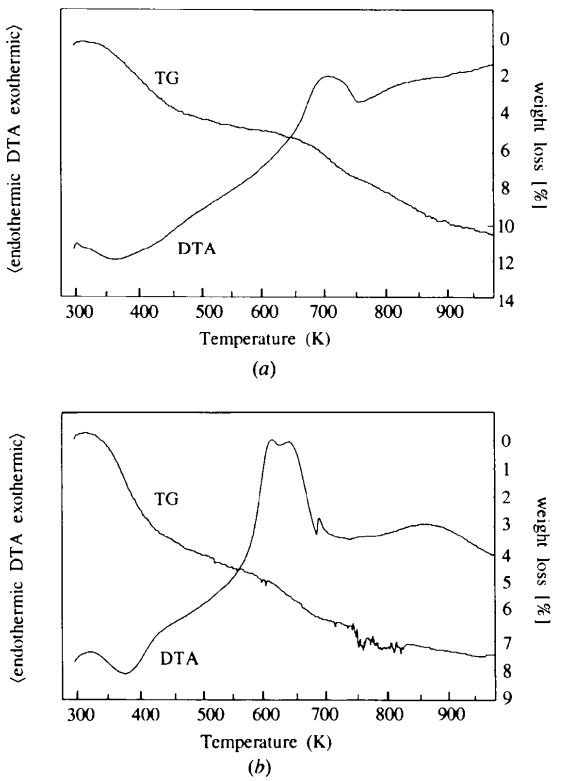

Fig. 1. Thermal reactions recorded by differential thermal analyses (DTA) and weight loss determined by thermogravimetry (TG): (*a*) Rho-I-5TMA; (*b*) Rho-II-5TMA.

Table 2. *Crystal data [space group, lattice constant a, volume V, framework density FD (no. of T atoms per 1000 Å^3), ellipticity parameter Δ_e] and residuals; for definitions see Weidenthaler, Fischer, Abrams & Hewat (1997), Table 3*

	Rho-I		Rho-II	
	Rho-I-5TMA X-ray	Rho-I-5TMA Neutron	Rho-II-5TMA X-ray	Rho-II-5TMA Neutron
Space group	*Im*$\bar{3}$*m*	*Im*$\bar{3}$*m*	*Im*$\bar{3}$*m*	*Im*$\bar{3}$*m*
a (Å)	15.0542 (2)	15.0467 (4)	15.0574 (2)	15.0761 (5)
V (Å^3)	3411.7	3406.6	3413.9	3426.6
FD (10^{-3} Å^{-3})	14.07	14.09	14.06	14.01
A (Å)	3.89	3.93	3.77	3.89
Δ_e	1	1	1	1
R_{wp}	0.094	0.034	0.118	0.037
R_B	0.062	0.099	0.050	0.099

Table 3. *Restrained settings in the DLS refinements; N—C=1.4535, C—C=2.3870 Å, C—N—C=110.4°, N—D=1, T—O=1.6331, O—O=2.6668 Å*

Sample	T—O	O—O	N—C	C—C	C—N—C	N—D
Rho-I-5TMA X	*	*	*	*	*	
Rho-I-5TMA N			*	*	*	*
Rho-II-5TMA X			*	*	*	
Rho-II-5TMA N			*	*	*	*

2.2.1. *Rho-I-5TMA X.*

The framework structure of the zeolite was refined using initially the coordinates for space group *Im*$\bar{3}$*m* from Fischer, Baur, Shannon, Staley, Abrams, Vega & Jorgensen (1988). Fourier and Difference-Fourier analyses revealed positions in 0,0,0.27, 0.05,0.07,0.21 and 0,0,0.33. The first two positions have a distance of *ca* 1.6 Å to each other, which approximately corresponds to an N—C bond in TMA. Therefore, N was assigned to 0,0,0.27 and the C atom to the general position in 0.05, 0.07, 0.21. This gives an arrangement around N with two C atoms symmetrically related *via* the mirror plane with a C—N—C angle approximately corresponding to the tetrahedral angle. The 0,0,0.33 position was assumed to be occupied by water (*W*1) molecules. The close distances to Cs and N atoms are avoided by the statistical occupation of these sites. Refinements with fixed occupancies of five N and ten C atoms per unit cell lowered the residuals from R_{wp} = 0.787 to 0.514 and R_B from 0.730 to 0.454. Geometric considerations yielded the

Table 4. *Atom positions in fractional coordinates*

Isotropic displacement factors (Å^2) and occupancies given in number of atoms per unit cell.

Sample position (Å^2)	Atom	x	y	z	B (Å^2)	Atoms per unit cell	Wyckoff position
Rho-I-5TMA X	Si/Al	1/4	0.1021 (1)	$\frac{1}{2}-y$	1.43 (4)	39/9	(48*i*)
Rho-I-5TMA N	Si/Al	1/4	0.1026 (2)	$\frac{1}{2}-y$	1	39/9	(48*i*)
Rho-II-5TMA X	Si/Al	1/4	0.1034 (1)	$\frac{1}{2}-y$	1.68 (5)	42/6	(48*i*)
Rho-II-5TMA N	Si/Al	1/4	0.1004 (2)	$\frac{1}{2}-y$	1.38 (6)	42/6	(48*i*)
Rho-I-5TMA X	O1	0	0.2187 (3)	0.3776 (2)	1.8 (1)	48	(48*j*)
Rho-I-5TMA N	O1	0	0.2207 (2)	0.3796 (2)	1.28 (3)	48	(48*j*)
Rho-II-5TMA X	O1	0	0.2147 (3)	0.3829 (3)	3.9 (2)	48	(48*j*)
Rho-II-5TMA N	O1	0	0.2185 (2)	0.3805 (2)	1.02 (4)	48	(48*j*)
Rho-I-5TMA X	O2	0.1631 (2)	x	0.3704 (3)	3.3 (2)	48	(48*k*)
Rho-I-5TMA N	O2	0.1661 (2)	x	0.3701 (2)	3.00 (6)	48	(48*k*)
Rho-II-5TMA X	O2	0.1668 (2)	x	0.3741 (3)	3.6 (2)	48	(48*k*)
Rho-II-5TMA N	O2	0.1653 (2)	x	0.3756 (3)	2.05 (6)	48	(48*k*)
Rho-I-5TMA X	Cs	0	0	0.4074 (8)	5	1.2 (1)†	(12*e*)
Rho-I-5TMA N	Cs	0	0	1/2	5	0.2	(6*b*)
Rho-II-5TMA X	Cs	0	0	0.423 (1)	5	0.8 (1)†	(12*e*)
Rho-II-5TMA N	Cs	0	0	1/2	5	0.7	(6*b*)
Rho-I-5TMA X	*W*1	0	0	0.324 (1)	5	5.9 (1)†	(12*e*)
Rho-II-5TMA X	*W*1	0	0	0.333 (1)	5	6.2 (1)†	(12*e*)
Rho-I-5TMA X	*W*3/*X**‡	0.1603 (7)	x	x	5	8.4 (2)	(16*f*)
Rho-II-5TMA X	*W*3/*X**‡	0.131 (7)	0.073 (1)	0.186 (1)	5	14.5 (2)	(96*l*)
Rho-II-5TMA N	*W*3/*X**‡	0.0994 (6)	x	0.1658 (8)	5	15.3 (2)	(48*k*)
Rho-I-5TMA X	*W*4/*X**‡	0.0551 (5)	x	0.1665 (5)	5	15.7 (1)	(48*k*)
Rho-I-5TMA N	*W*4/*X**‡	0.0952 (8)	0.057 (1)	0.1474 (6)	5	16.1 (3)	(96*l*)
Rho-II-5TMA X	*W*4/*X**‡	0.083 (1)	x	0.043 (3)	5	5.3 (1)	(48*k*)
Rho-I-5TMA X	N	0	0	0.2793 (7)	5	5	(12*e*)
Rho-I-5TMA N	N	0	0	0.2698 (4)	5	5	(12*e*)
Rho-II-5TMA X	N	0	0	0.2677 (8)	5	5	(12*e*)
Rho-II-5TMA N	N	0	0	0.2772 (5)	5	5	(12*e*)
Rho-I-5TMA X	C1	0	0.0918 (4)	0.2481 (7)	5	5	(48*j*)
Rho-I-5TMA N	C1	0	0.0912 (4)	0.2362 (5)	5	5	(48*j*)
Rho-II-5TMA X	C1	0	0.0915 (5)	0.2361 (8)	5	5	(48*j*)
Rho-II-5TMA N	C1	0	0.0912 (4)	0.2455 (6)	5	5	(48*j*)
Rho-I-5TMA X	C2	0.0793 (4)	0.0454 (4)	0.2481 (7)	5	10	(96*l*)
Rho-I-5TMA N	C2	0.0793 (2)	0.0466 (4)	0.2362 (5)	5	10	(96*l*)
Rho-II-5TMA X	C2	0.0454 (5)	0.0792 (2)	0.2361 (8)	5	10	(96*l*)
Rho-II-5TMA N	C2	0.0454 (5)	0.0792 (2)	0.2455 (6)	5	10	(96*l*)
Rho-I-5TMA N	D	0	0	0.3362 (5)	5	5	(12*e*)
Rho-II-5TMA N	D	0	0	0.3434 (6)	5	5	(12*e*)

† Occupancy constrained to give a total of 12 atoms in the sum of Cs, *W*1 and TMA with a fixed number of five TMA molecules. ‡ *X** in the dehydrated samples the *X* position is assigned to n.f.a. species. Statistical distribution of water molecules and n.f.a. species (x) on the same site is assumed. Refinement is based on 0 scattering factor only.

remaining C1 position in 0, 0.09, 0.21 for the tetrahedral coordination of C around N. The occupancy was held fixed to five atoms per unit cell in the refinements. Additional maxima in the difference-Fourier maps were assigned to Cs and two more water positions *W*3 and *W*4, which yielded residuals of R_{wp} = 0.229 and R_B = 0.210 in the refinements. Final refinements including all atomic parameters and profile values with the DLS restraints given in Table 3 yielded the final results listed in Table 4.

2.2.2. *Rho-I-5TMA N.* The framework structure of the dehydrated sample of series I could be refined without DLS constraints on interatomic distances. The neutron diffraction profiles (Fig. 2) show that the sample apparently does not decompose into two separate phases of zeolite rho, as observed for the MMA zeolites. Difference-Fourier analyses (Fig. 3) of the single phase intensities immediately revealed the TMA positions with N on 0,0,0.22. The position in 0,0,0.33 was assigned to the D atom, which complements the tetrahedral coordination of the three methyl groups around N. The N—D distance was constrained to 1 Å in the refinements. The D atoms of the methyl groups could not be determined. As in the case of the neutron diffraction analyses of the dehydrated MMA zeolites, an additional peak appeared in the difference-Fourier map, which could not be assigned to any of the framework or nonframework positions. For reasons discussed before, the most probable interpretation is an assignment to nonframework aluminum species (n.f.a.) which have been formed upon deammoniation of the NH_4 precursor zeolite, which induces considerable dehydroxylation and dealumination of the aluminosilicate framework. Incor-

poration of this position *X* with the scattering length of oxygen improved the final residuals R_{wp} from 0.042 to 0.034 and R_B from 0.123 to 0.099.

2.2.3. *Rho-II-5TMA X.* As in the case of the MMA and DMA zeolites of series II, the chabazite impurity was treated as a second phase in the refinements with a contribution of *ca* 4 mol % calculated from the refined scale factors. Only the lattice parameters were refined and all structural data were taken from Smith, Rinaldi & Dent Glasser (1963) and transformed into the hexagonal setting. Difference-Fourier calculations revealed that the N and C1 atoms of the TMA molecule reside in 0,0,0.28 and 0,0.05,0.25. The second C atom could not be located from the Fourier calculations. It has been determined by geometric considerations and refined with prescribed distances for a tetrahedral coordination around N. Incorporation of the second C position lowered the residuals R_{wp} from 0.207 to 0.188 and R_B from 0.201 to 0.148, which confirms a correct assignment. Additional electron densities were assigned to water positions. Occupancies for the TMA atoms were fixed to yield five molecules per unit cell. The occupancies of the water molecules and the Cs atom were refined yielding 26 H_2O per unit cell and 0.8 Cs atoms per unit cell, which are very close to the 22 H_2O and 0.7 Cs determined from thermal and wet chemical analysis.

2.2.4. *Rho-II-5TMA N.* Following the same procedure as in the hydrated sample described above, the atomic positions of the TMA molecule could be directly determined from the Fourier calculations, including the two crystallographically independent C atoms of the methyl groups and the D atom as the fourth ligand in the tetrahedral group. However, the D atoms of the CD_3 groups could not be determined. The chabazite fraction was calculated with a 3% contribution, which differs by 1% from the X-ray determination, but is within the error margins of the refinements. Deviations between observed and calculated intensities (Fig. 2) are mainly due to the chabazite contributions.

The final fits between observed and calculated intensities are shown in Fig. 2, the results of the refinements are listed in Table 4, selected interatomic distances and angles are given in Table 5.

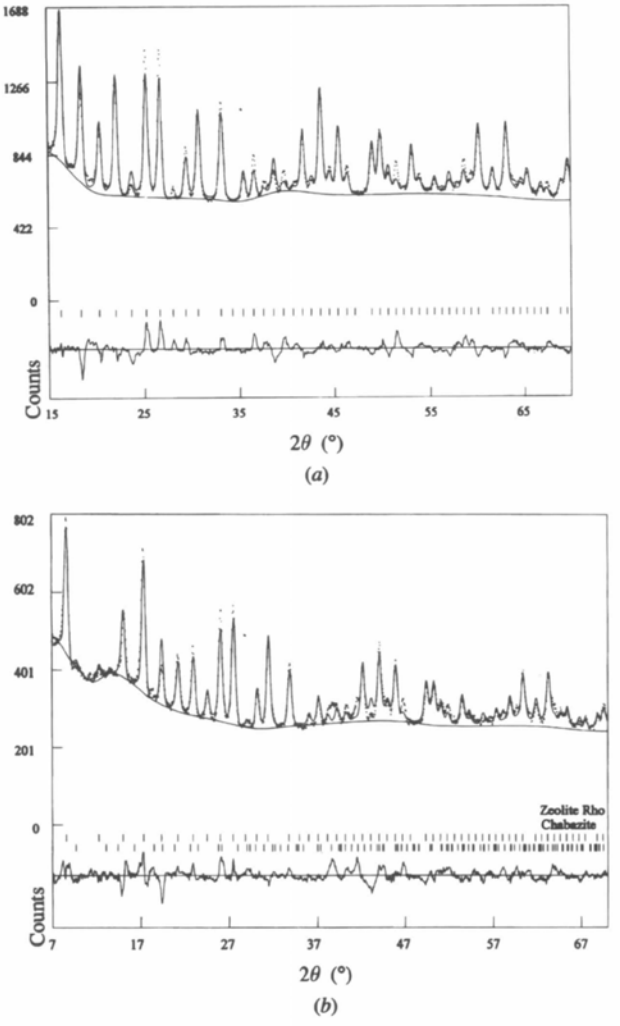

Fig. 2. Observed (+) and calculated (solid line) neutron intensities with difference plot underneath. Peak positions are indicated by tick marks: (*a*) Rho-I-5TMA; (*b*) Rho-II-5TMA.

3. Discussion

3.1. *The effect of methylamine loadings on the (Si,Al)O_2-framework*

All samples exhibit a centrosymmetric structure in $Im\bar{3}m$, which does not allow the extreme framework distortions known from the modifications crystallizing in the noncentrosymmetric space group $I\bar{4}3m$. The minimum channel apertures fit exactly into the plot of

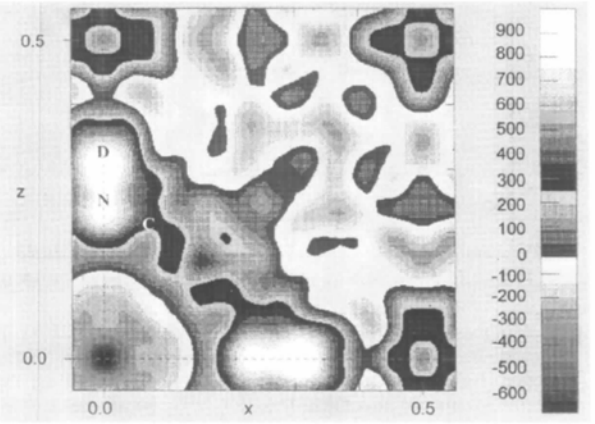

Fig. 3. Difference-Fourier maps of Rho-I-5TMA in the layer $y = 0$ with F_{obs} values from X-ray and neutron diffraction data and F_{calc} values from the corresponding refinements of framework atoms. The highest maximum is scaled to 999. The positions of the molecules are indicated by the labels for the N and C atoms.

Table 5. *Selected interatomic distances (Å) and angles (°)*

	Rho-I		Rho-II	
	5TMA X-ray	5TMA Neutron	5TMA X-ray	5TMA Neutron
T—O1	1.637 (4) 2×	1.627 (4) 2×	1.658 (5) 2×	1.612 (5) 2×
T—O2	1.651 (3) 2×	1.636 (3) 2×	1.611 (4) 2×	1.649 (3) 2×
Mean	1.644 (4)	1.632 (4)	1.635 (5)	1.631 (4)
O1—T—O1	115.7 (2)	112.7 (2)	109.7 (3)	115.0 (3)
O1—T—O2	104.4 (1) 2×	107.7 (1) 2×	106.3 (2) 2×	106.9 (2) 2×
O1—T—O2	111.1 (2) 2×	110.5 (2) 2×	111.9 (2) 2×	109.2 (2) 2×
O2—T—O2	110.4 (2)	107.6 (2)	110.8 (2)	109.8 (2) 2×
Mean	109.5 (2)	109.5 (2)	109.5 (2)	109.5 (2)
N—O1	3.609 (5) 4×	3.710 (3) 4×	3.669 (7) 4×	3.643 (4) 4×
N—O2	3.734 (5) 4×	3.843 (4) 4×		
C1—O1	2.730 (9)	2.908 (8)	2.89 (1)	2.797 (8)
C1—O2	3.252 (7)	3.402 (6)	3.451 (8)	3.363 (6)
C2—O2	2.851 (9)	3.000 (7)	3.07 (1)	2.968 (8)
C2—O1	2.945 (8)	3.11 (6)	3.084 (9)	3.003 (7)

the corresponding values from the MMA and DMA rho's (Fig. 4). While the smaller MMA molecules have a tremendous influence on the lattice parameters, the framework structure is stabilized in its centrosymmetric form by the larger DMA and TMA molecules. Similar lattice parameters and apertures are also achieved by H-rho's (Baur, Fischer, Shannon, Staley, Vega, Abrams, Corbin & Jorgensen, 1987; Fischer *et al.*, 1988), which do not contain huge amounts of large cations. The methylamines exhibit strong bonds with the framework atoms causing the distortions in the MMA-rho zeolites. The larger DMA and TMA molecules obviously block the transition from the centrosymmetric round channels to the noncentrosymmetric elliptically distorted channels. Similar effects can be observed for NH_4-rho zeolites, which fit exactly into the curve representing the channel openings in Fig. 4. If the zeolite is loaded by less than five molecules of TMA (Meyer, 1994), the crystal structure transforms to its noncentrosymmetric form.

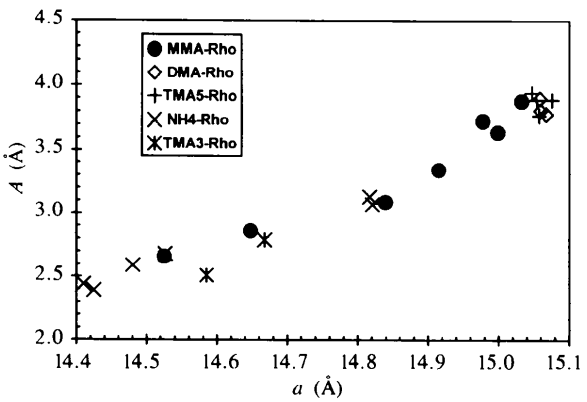

Fig. 4. Minimum apertures based on ionic oxygen (r = 1.35 Å) of the eight-ring channels defined by the eight-ring diameter in the direction [100] for the centrosymmetric structures and [110] for the noncentrosymmetric structures. Data for NH_4-rho are taken from McCusker (1984), Fischer, Baur, Shannon, Parise, Faber & Prince (1989), Corbin, Abrams, Jones, Eddy, Harrison, Stucky & Cox (1990) and Bieniok & Baur (1993). Zeolites with minor amounts of ammonium are not considered. The data points for the zeolite rho loaded with three molecules of TMA have been taken from Meyer (1994).

3.2. *The water molecules*

Water molecules have been determined to reside in the *W*1, *W*3 and *W*4 sites. The *W*2 molecules have been found in samples with the smaller methylamines, but they do not occur in the TMA zeolites. The crystal chemical environment is similar to the corresponding water sites described in the preceding papers (Weidenthaler, Fischer & Abrams, 1997; Weidenthaler, Fischer, Abrams & Hewat, 1997). In the fully hydrated samples the *W*1 molecules have a closest contact to *W*4 [Rho-I-5TMA X] or *W*3 molecules [Rho-II-5TMA X] and they are weakly bonded to framework O atoms with 3.39 and 3.32 Å, respectively. The *W*3 molecules have *W*4 molecules as nearest neighbors and the shortest distances to framework O2 atoms. The *W*4 molecules are coordinated by nonframework atoms only. In the dehydrated sample positions close to the *W*3 and *W*4 sites of the hydrated zeolites have been assigned to n.f.a. species with the uncertainties discussed in the MMA-rho paper. It cannot be stated unambiguously that the sample is not contaminated by water introduced by a leak in the sample container. However, it seems to be unlikely that a water contamination has occurred in all four samples with approximately similar numbers of atoms per unit cell for the MMA and TMA refinements, respectively (12.0 in Rho-I-5MMA N and 10.7 in Rho-II-5MMA N, 16.1 in Rho-I-5TMA N and 15.3 in Rho-II-5TMA N).

3.3. *The TMA molecules*

The constraints on the intramolecular distances by prescribed values do not affect the orientation of the methylamines with respect to the zeolite framework. Free rotations and translations of the molecules are permitted, which is sufficiently accurate for the description of the molecules' positions in the zeolite host. As shown in Fig. 5, the TMA molecule resides on the central axis (x, 0, 0) through the α-cage. The N and D atoms are located on that axis with the D atom pointing to the center of the single eight-ring. The remaining C atoms complete the tetrahedral arrangement with C1 on the mirror plane and the two C2 atoms at both sides of the mirror plane. The highest possible symmetry of the TMA molecule is $3m$, which is inconsistent with the site symmetry $4m.m$ of the x, 0, 0 position. Consequently, the C2 atoms cannot be placed on the diagonal mirror planes x, x, 0. The molecule shown in Fig. 5 represents just one out of four possible orientations of the molecule. The bond distances of the C atoms to framework O atoms are given in Fig. 5. The closest contact to the framework atoms is between the C1 and O1 atoms with distances averaged for all TMA samples of 2.83 Å. Somewhat

longer distances (~ 2.90 Å) could be achieved by a shift of the N atom away from the central axis x, 0, 0. This, however, cannot be verified in the refinements due to the high disorder in the statistical distribution of the TMA atoms. An offset of the C1 atom from the mirror plane permitting a rotation of the molecule about the central axis is rather unlikely since this would cause a decrease in the C2—O distances.

In contrast to the observations in the MMA loaded samples, dehydration does not cause a phase transition and reorientation of the TMA molecules nor does it cause the decomposition into two phases, as observed for the MMA-rho's. Obviously, the larger TMA molecule is less mobile and stabilizes the structure against thermal effects.

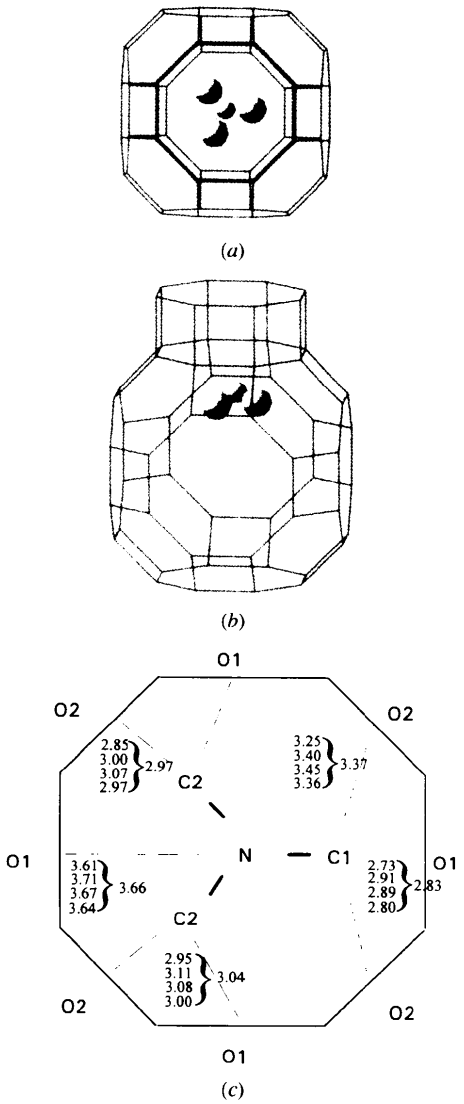

Fig. 5. Projection of the framework structure of Rho-I-5TMA as a skeleton model with the TMA molecule close to the single eight-ring. The large circles represent the C atoms (methyl groups), the smaller circles the N atoms. The α-cage with one double eight-ring and only one molecule in one orientation is shown. (a) Top view; (*b*) side view; (*c*) schematic representation with distances to framework O atoms (from top to bottom: Rho-I-5TMA X, Rho-I-5TMA N, Rho-II-5TMA X, Rho-II-5TMA N).

3.4. *Comparison of zeolites rho loaded with ammonium and its methylamine derivatives*

The plot of minimal channel apertures of all ammonium and methylamine-loaded zeolite rho in Fig. 4 shows that the increase in the channel openings is almost a linear function of the lattice constants for both the noncentrosymmetric and centrosymmetric entries. The slope is somewhat steeper for the centrosymmetric zeolite rho's above *ca* 14.8 compared with the values for the noncentrosymmetric zeolite rho.

The only report on methylamine-loaded zeolite rho except our studies is given by Meyer (1994). The samples studied by Meyer (1994) are reported to have a very unusual chemical composition with a Cs content higher than the Na content and with an Si:Al ratio of 4.6:1 compared with the universally reported zeolite compositions with higher Na contents and with an Si:Al ratio of *ca* 3:1. Therefore, the samples studied here cannot be compared directly with the results reported for the TMA-rho by Meyer (1994). There, the TMA molecules are located off the fourfold axis with the N atoms in the general position x, y, z. This yields close contacts of N and O atoms in the four-ring with N—O distances between 2.68 and 2.77 Å in two determinations. These values correspond to the lower range of distances observed for NH_4-rho, whereas the methylamine derivatives show an approximately linear increase as a function of their size expressed by the number of methyl groups in Fig. 6. It should be noted that Meyer (1994) describes neutral $N(CH_3)_3$ species, while the TMA molecules studied here have a cationic charge according to $H—N(CH_3)_3^+$. Consequently, their crystal chemical behavior may be different.

It becomes evident from these studies of methylamine-loaded zeolites that the TMA molecules

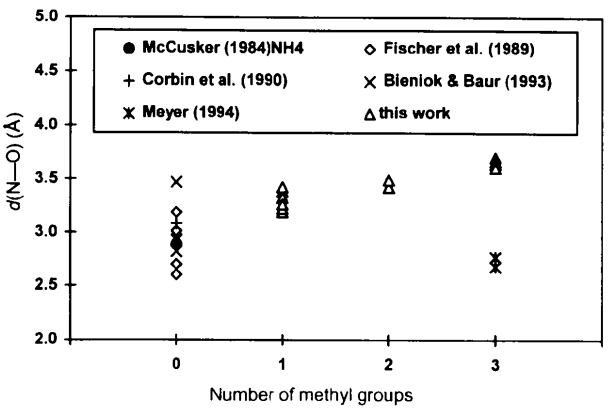

Fig. 6. Shortest distances between N atoms and framework O atoms as a function of the number of methyl groups involved in the methylamines. Entries for MMA- and DMA-rho are from parts I and II of this series (Weidenthaler, Fischer & Abrams, 1997; Weidenthaler, Fischer, Abrams & Hewat, 1997).

reside in a fixed position, whereas the MMA molecules migrate from the α-cage into the double eight-rings. The catalytical reaction of methanol with ammonia inside the cages of zeolite rho yields simultaneously MMA, DMA and TMA. Since these reactions were carried out with the catalytically active hydrogen forms of the zeolite activated at elevated temperatures, a similar crystal chemical behavior of the methylamine molecules was expected. Therefore, the observations obtained in this series of studies might be the key to the understanding of the catalytic behavior of zeolite rho.

This work was supported by the Deutsche Forschungsgemeinschaft under grant Fi442/2. The Heisenberg fellowship to RXF is gratefully acknowledged. Computing time was provided by the Zentrum für Datenverarbeitung, University of Mainz. We thank U. Ciesla and W. Schmidt (University of Frankfurt) for the thermal analyses, N. Groschopf (University of Mainz) for support with the chemical analyses and W. H. Baur (University of Frankfurt) for his careful reading and numerous comments on the manuscript.

References

Abrams, L., Corbin, D. R. & Keane, M. Jr (1990). *J. Catal.* **126**, 610–618.

Baur, W. H., Fischer, R. X., Shannon, R. D., Staley, R. H., Vega, A. J., Abrams, L., Corbin, D. R. & Jorgensen, J. D. (1987). *Z. Kristallogr.* **179**, 281–304.

Bieniok, A. & Baur, W. H. (1993). *Acta Cryst.* B**49**, 817–822.

Blake, A. J., Ebsworth, E. A. V. & Welch, A. J. (1984). *Acta Cryst.* C**40**, 413–415.

Corbin, D. R., Abrams, L., Jones, G. A., Eddy, M. M., Harrison, W. T. A., Stucky, G. D. & Cox, D. E. (1990). *J. Am. Chem. Soc.* **112**, 4821–4830.

Fischer, R. X., Baur, W. H., Shannon, R. D., Parise, J. B., Faber, J. & Prince, E. (1989). *Acta Cryst.* C**45**, 983–989.

Fischer, R. X., Baur, W. H., Shannon, R. D., Staley, R. H., Abrams, L., Vega, A. J. & Jorgensen, J. D. (1988). *Acta Cryst.* B**44**, 321–334.

Keane, M. Jr, Sonnichsen, G. C., Abrams, L., Corbin, D. R., Gier, T. E. & Shannon, R. D. (1987). *Appl. Catal.* **32**, 361–366.

McCusker, L. B. (1984). *Zeolites*, **4**, 51–55.

Meyer, J. (1994). Phasencharakterisierung im ternären System Zeolith RHO–Trimethylamin–Wasser. Ph.D. thesis, Technische Hochschule Darmstadt.

Shannon, R. D., Keane, M. Jr, Abrams, L., Staley, R. H., Gier, T. E., Corbin, D. R. & Sonnichsen, G. C. (1988). *J. Catal.* **113**, 367–382.

Smith, J. V., Rinaldi, F. & Dent Glasser, L. S. (1963). *Acta Cryst.* **16**, 45–53.

Weidenthaler, C., Fischer, R. X. & Abrams, L. (1997). *Acta Cryst.* B**53**, [SE0200].

Weidenthaler, C., Fischer, R. X., Abrams, L. & Hewat, A. (1997). *Acta Cryst.* B**53**, [SE0199].